

## Implementation and Design of Low-cost Microfluidic device to separate blood plasma using Rapid Prototyping Method.

S. Pradeep Kumar<sup>1\*</sup>, N. Shanmugasundaram<sup>2</sup>, E.N.Ganesh<sup>3</sup>, M.Suganiya<sup>4</sup>

<sup>1</sup> Assistant Professor, Department of Electrical and electronics Engineering, Vels Institute of Science Technology and Advanced Studies, Chennai- 600117

<sup>2</sup> Associate Professor, Department of Electrical and electronics Engineering, Vels Institute of Science Technology and Advanced Studies, Chennai- 600117

<sup>3</sup> Dean, School of Engineering, Vels Institute of Science Technology and Advanced Studies, Chennai- 600117

<sup>4</sup> Junior Research Fellow, Department of Computer Science Engineering, Vels Institute of Science Technology and Advanced Studies, Chennai- 600117

[pradeep88.se@velsuniv.ac.in](mailto:pradeep88.se@velsuniv.ac.in)

### Abstract

This study applied a low-cost and rapid fabrication technique using a cutting plotter to address the prototype of microfluidic device for blood plasma separation. Microchannels were carved into commercial clear plastic films made from polyvinylchloride with plasticizer and polyethylene terephthalate. The results revealed the capability to create negative microchannels whose sizes less than 100  $\mu\text{m}$  on to the films. The channel distortion occurred on the horizontal cutting axis more than the vertical one. The final microfluidic device established the drift or cell-free layer (CFL) enhanced at downstream channel about 10  $\mu\text{m}$  thick, which provided the region to separate blood plasma.

**Key Words:** *Microfluidics / Rapid Prototyping / Cutting plotters / Cell-free layer*

### 1. INTRODUCTION

The development of microfluidics has grown rapidly over the past decade. Microfluidic devices ( $\mu\text{F}$ ) have been widely applied in many fields including scientific, industrial, and biomedical fields. Most of the microfluidic devices are made from the method based on a microelectronic fabrication technique, called photolithography, on

Materials like glass, quartz, or silicon and poly(dimethylsiloxane) (PDMS). However, this technique is quite complicated and required expensive apparatus. For developing countries, the major challenge is how to fabricate the devices in a rapid, simple, and inexpensive way. Numerous of unconventional low cost fabrication techniques have been presented, such as patterning SU-8 photoresist and wax onto papers[1], x-y desktop plotting[1] and xurography[2]–[4], to address these challenges. Some drawbacks, e.g., less precise, unsmooth surface, low resolution, appeared among the fabrication methods. Xurographic prototyping is a useful and inexpensive research tool to focus on the microfluidic device development before moving to higher qualitative techniques[2]. The hardware resolution is specified by the resolution of motors, while the software resolution is limited with the resolution down to 25  $\mu\text{m}$  of step size[2]. Craft cutting plotters, with thin cutting blade, are presented to carve microchannels directly to the surface of various materials[2]. This easy-to-prototype, inexpensive, method enhances the

microchannel fabrication without clean room facilities. This study applied the low-cost fabrication technique using a cutting plotter with inexpensive materials of transparent plastic films to address the microfluidic

device for blood plasma separation. Because blood samples are usually separated into blood plasma before performing blood tests, separating plasma on microfluidic devices would be a challenge. Many researches *Fig. 1. Layout of microchannel for the microfluidic cell focusing device., where  $w_c$  is the width of the main channel upstream and downstream. The length ( $L$ ) and width ( $w$ ) were geometry of rectangular constriction channel.* reported that manipulating geometry of microchannel affected the hydrodynamic separation of red blood cells (RBCs) and plasma. Faivre *et al.* presented the manipulation in width ( $w$ ) and length ( $L$ ) of the rectangular constriction channel shown in Fig.1 to enhance CFL or drift  $d$  at downstream[5]. Then, the enhanced CFL was applied to separate blood plasma in microfluidic devices[6]. This passive technique was possible to extract plasma 10-25% out of the injected volume, with an excellent purity, low contamination rate, even for 1:10 and 1:20 diluted blood[6], [7]. For this study, the microchannel based on the xurographic technique was investigated. Finally, the prototype of the microfluidic device for enhancing the CFL thickness, which provided the region to separate blood plasma, was developed.

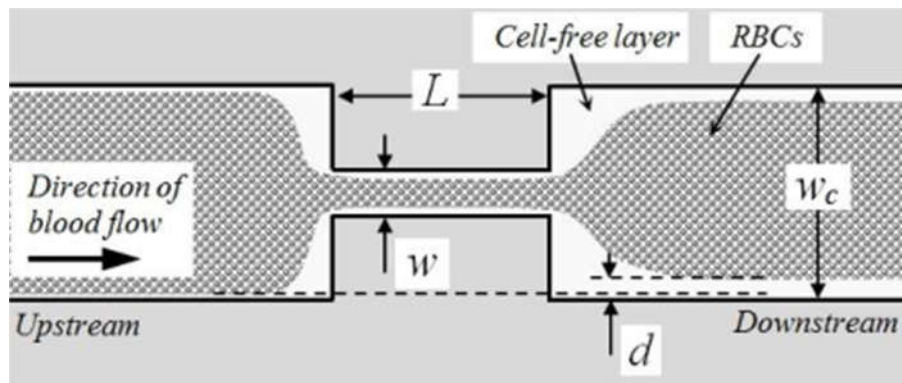


*Figure 1. Layout of microchannel for the microfluidic cell focusing device., where  $w_c$  is the width of the main channel upstream and downstream. The length ( $L$ ) and width ( $w$ ) were geometry of rectangular constriction channel.*

## 2. MATERIALS AND METHODS

### 2.1. Choice of materials

Two types of clear plastic films, Polyvinylchloride with plasticizer (PVC) and Polyethylene terephthalate (PET) were selected for carved material in this study. Their advantages also include lightweight, flexibility, smooth surface, good optical transparency and inexpensive material. The A4 sheet of the films which normally used for presentation and laser printing were purchased from Office Mate Co., Ltd. Thailand (~\$10 per 100 sheets). Although the nominal thicknesses of both films are ~100  $\mu\text{m}$ , other mechanical properties are different. Young's modulus of PVC and PET films are 25-1600 MPa and 2100-3100 MPa, respectively. Moreover their thermal properties are also different.

### 2.2. Fabrication of clear plastic microfluidic devices

The craft cutting plotter (Silhouette Cameo Silhouette America Inc.), with commercial thin cutting blade and cutting mat, was introduced to carve microchannels directly onto the surface of the plastic films. Computer-aided design software (Solid Edge 2D Drafting ST6 Free License, Siemens Product Lifecycle Management Software Inc.) was used to design the layouts of microchannels. The layouts were saved as the DXF file format and imported to the plotter software of Silhouette Studio® V3 for cutting control. The plotter software has the ability to assign cutting parameters such as cutting speed, cutting force, cutting style and etc. The rapid fabrication processes from carving

the designed layout to the completed chip have shown in Fig. 2. A piece of plastic film was adhered onto a recyclable cutting mat and then carved the designed layout. After peeling off the layer from the mat, the layer was sealed using double layers of thermal laminating films (Laminating pouch film 125  $\mu\text{m}$  thick, Value Choice Office Mate Co., Ltd.) with pre-cut inlets and the outlets to finish the microfluidic chip. A roller thermal laminator was preheated at 140°C before the chip bonding. Finally, a custom acrylic chip holder, with tubing connectors and rubber plugs of continuous ink supply systems (CISS) for an inkjet printer, polyethylene tubing (I.D. 0.58 mm, O.D. 0.965 mm), was used to connect the fabricated microfluidic chip to a syringe (1 mL, Terumo Inc.) during experiments.

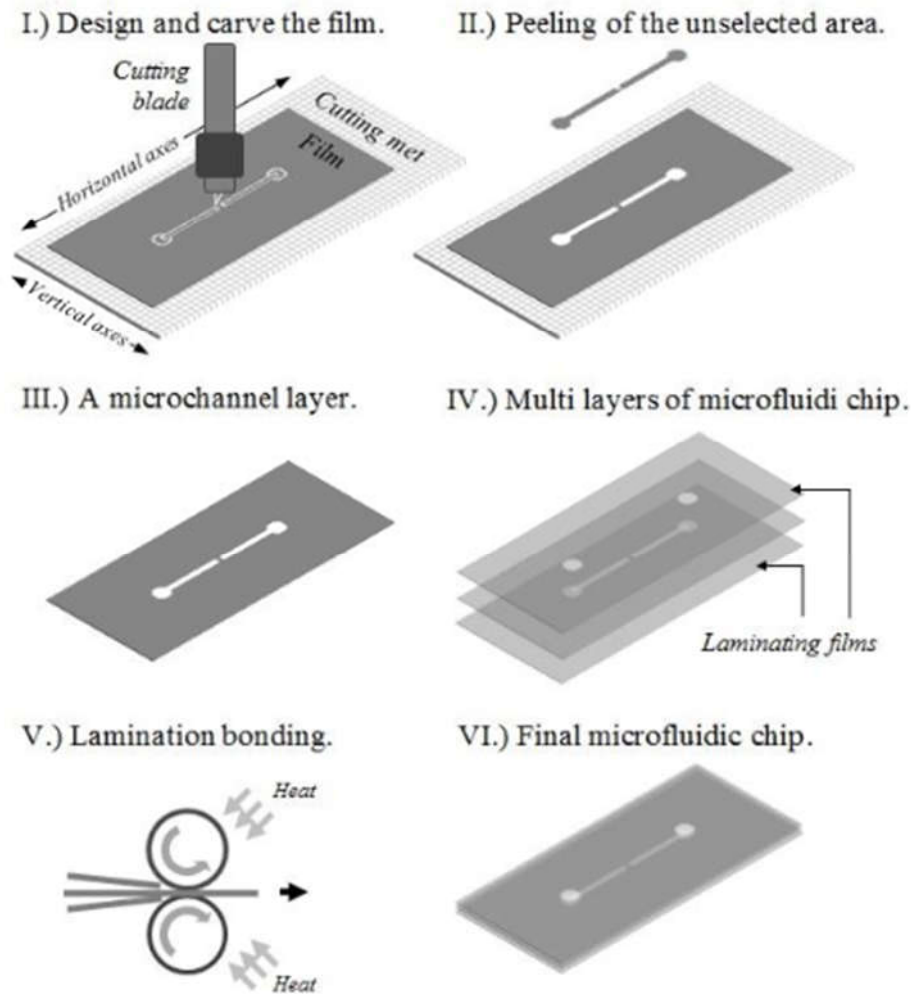


Figure 2. Illustration of the microfluidic fabrication

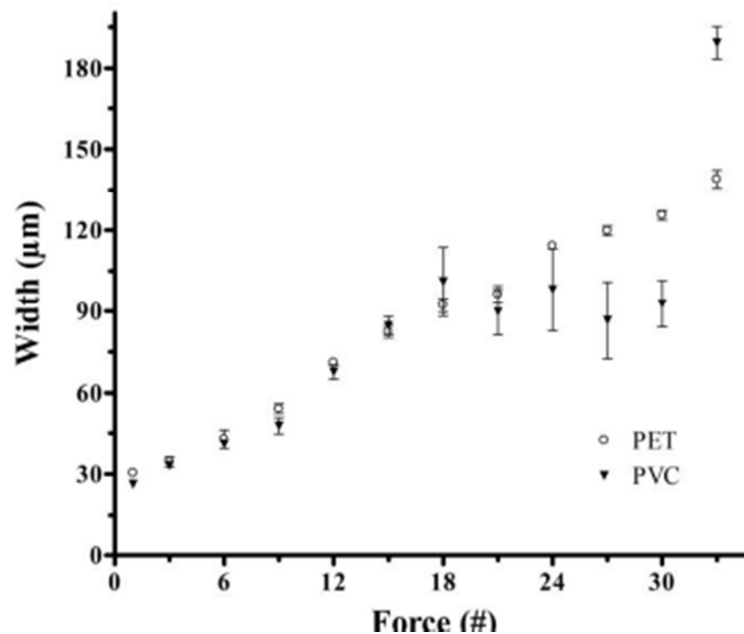


Figure 3. Plot of microchannel width specified by different cutting forces on to both plastic films.

## 2.2. Blood sample preparation

Blood sample used in the experiments was obtained from a healthy hamster in EDTA tubes (Vacutainer, BD). The hematocrit percentage of blood sample was 41%. The sample was diluted to 1:10 by normal saline solution (NSS) with heparin (IP, 1000 USP/mL). Experiments were conducted on the same day of blood collection.

## 2.3. Experimental procedures

### 2.3.1. Characterization of microchannels

To investigate microchannel feature size, the straightcarving lines of 10-mm-long at various applied forces (Level 1 to 33 as maximum cutting force of 210 gf) and the rectangular-carving patterns of 10 mm long and 100 µm to 1000 µm width were cut onto the surface of both types of plastic films. The microstructures on the surfaces were captured using a CCD camera (D90, Nikon) attached to a light microscope (CKX41, Olympus). Finally, the feature size was measured, at the microchannel positions of 2.5, 5.0 and 7.5 mm length, using the image processing software of ImageJ.

### 2.3.2. Enhancement of the downstream CFL after the constriction

The layout of the microfluidic cell focusing device has shown in Fig. 1. This device geometry and drift parameter  $d$  were reported by Faivre *et al.*[5] as shown in equation (1) below. The following layout:  $L=300$  µm,  $w_c=500$  µm,  $w=100$  µm was designed with the predicted drift  $d$  more than 10 µm using equation (1). The channel height was 100 µm.

$$d = 0.26 + 0.24 \frac{LW_c}{W^2} \quad (1)$$

The fluid flow in microchannels was controlled by a standard motor-driven pump with constant flow rate of 10 µL/min. Movies and images were taken with the CCD camera.

### 3. RESULTS AND DISCUSSION

The rapid fabrication steps from carving the designed layout to the completed chip was able to be finished less than ten minutes like previous study[4]: Step-I, a complete carving of individual microchannel layer can be done in a minute. Step-II, approving the microchannel layer with light microscope and image processing software would take ~5 min, and Step-III, the assembly and bonding of the final device spent ~1 min. Though, this low cost microfluidic chip could be achieved simply and rapidly, channel distortion and dimensional variation were typically occurred during the fabrication process. The smallest feature size of negative microchannel was obtained, approximately 30  $\mu\text{m}$  both on PVC and polyester films, by the minimum nominal applied force of level 1. As shown in Fig. 3, numerous feature size of microchannel occurred when applied the different cutting forces. The feature size was low deviation, when half cutting (not carving through out the thickness of materials). Die-cutting (carving through out) the PVC and PET films occurred when the applied force more than level 20 and 30, respectively. The different Young's modulus of plastic films affected the variability of feature size. However, this results have shown the capability to create negative microchannel whose size less than 100  $\mu\text{m}$  onto the PVC and PET. The negative microchannel size close to 50  $\mu\text{m}$  was found in PET and PVC shown in Fig. 4(a) and Fig. 4(b), respectively. Some roughness on the channel edge of both materials was appeared. It would be a key factor of the change in velocity profile as a result of increasing in average velocity[8]. Moreover, the laminated channels after bonding were narrower than the channels after cutting. This could be the bonding temperature of 140 $^{\circ}\text{C}$  was higher than the glass transition temperature (70- 80 $^{\circ}\text{C}$ ) so that the channels were creep during pressed. Despite these size changes, the laminated PET channel width in Fig. 4(c) was less deviated than that of PVC shown in Fig. 4(d). The thermal expansion property of the PET films promoted the stability over the PVC. The other bonding technique with glue[9] should be more suitable for the PVC. Although chip bonding with thermal laminating films affect the channel width on plastic, this technique provide rapid bonded in a minute.

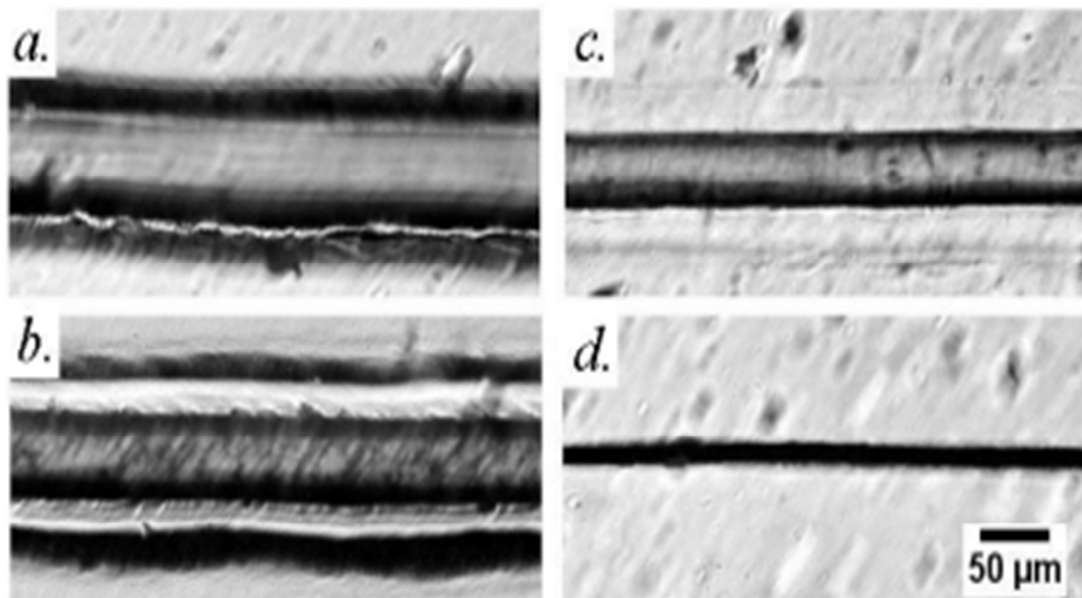


*Figure 4. Light microscope image of microchannel: the microchannels were obtained with an apply force level 9 onto the surface of PET(a) and PVC(b). Size of the microchannels on PET(c) and PVC(d) have changed after bonding with thermal lamination film*

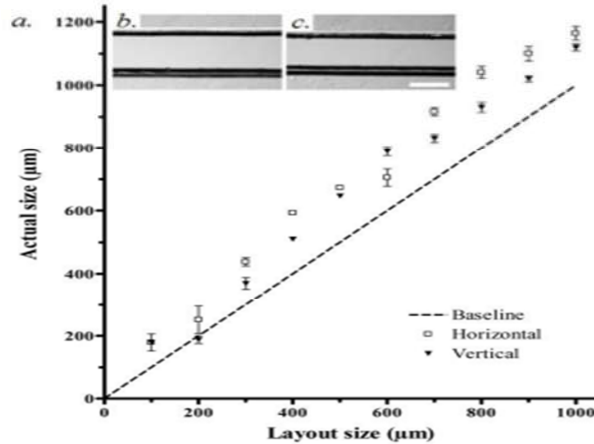


**Figure 5** shows the comparison of the actual sizes and the drawing sizes of the rectangular channels.

The other cutting study was the die-cutting 10 mm long of rectangular channels with varying the width sizes. The baseline (dash line) was the target width. However, the carved channels were overcut. It was found that the width of carved channels was about 10% more than which of the drawing. Because of the certain overcut, therefore drawing a layout 10% smaller than the target size could fit the final target width. The carving directions of rectangular channels were also examined, *i.e.* along the horizontal and vertical axes of the plotter. The plot of varies target channels on horizontal (opened square dots) and vertical cutting (rigid triangular dots) has also shown in Fig. 5(a). The phase contrast images in Fig. 5(b) and Fig. 5(c), were carved from 400  $\mu\text{m}$  layouts on PET films along the horizontal and vertical axes, respectively; however, the target channels were different. It found that cutting along the vertical axis was occurred less distorted than the horizontal one. Therefore, the more accurate channel size to the drawing would run in the vertical. This issue may cause by the different motion control system and motor drives on the horizontal and vertical or x-y axes. Normally, the cutting plotters work with different motion control system on x-y axes. For this study, the cutting plotter was a motion shaft control system on x-axis and a machine rollers system on y-axis. It was noticed that the channel distortion occurred on a single cutting plotter. It may provide the distortion less than 10% if working with other resolution plotters or higher grade cutting plotter. For approaching to a microfluidic device for blood plasma separation, the sample channel geometry reported by Faivre *et al.*[5] was chosen. Although the designed was very small constriction at 15  $\mu\text{m}$ , this research extended the constriction to 25 - 100  $\mu\text{m}$  like previous research[6] with the predicted drift  $d$  more than 10  $\mu\text{m}$ . The final device with the constriction area was shown in Fig. 6(a). The geometry of laminated microfluidic device was measured as  $L=396$   $\mu\text{m}$ ,  $w_c=558$   $\mu\text{m}$ , and  $w=78$   $\mu\text{m}$  as shown in small figure of Fig. 6(a). The constriction channel was slightly deformed at the end of the channel. As shown in Fig. 6(b), the picture of 1:10 diluted blood at the flow rate of 10  $\mu\text{L}/\text{min}$  was captured. The thin layer of CFL or the drift  $d$  of  $\square 10$   $\mu\text{m}$ , occurred clearly on a side of the downstream channel. The single side CFL could be affected by the deformation at the end of the constriction channel. However the channel deformation could not be control during the thermal lamination process. The uncontrollable channel deformation would possibly be improved by eliminating the surface roughness of the channel before bonding process.

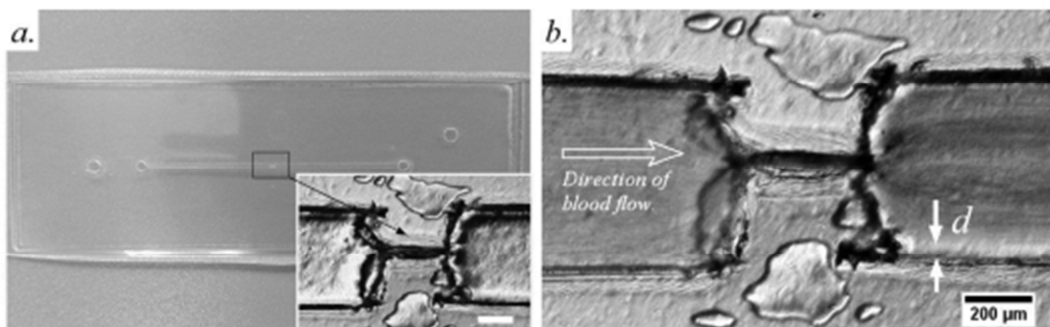


**Figure 6.** The final microfluidic chip for cell focusing(a) and the light microscope image of the microfluidic chip between blood flowing(b) through the channel. All scale bars are 200  $\mu\text{m}$ .

#### 4. CONCLUSION

The microfluidic fabrication processes from the drawing layout to the final device could be finish within ten minutes by xurography with thermal lamination films. The small negative microchannels, from 100  $\mu\text{m}$  to 30  $\mu\text{m}$  width, were fabricated with line carving. To fabricate bigger channels more than 100  $\mu\text{m}$ , die-cutting along the vertical axis was applied to obtain more accurate feature sizes than the horizontal one. However the actual microchannels were distorted 10% more than the drawing ones. The cell focusing chip using this fabrication technique was presented. Despite the uncontrollable channel deformation, the enhanced CFL at downstream was  $\square 10 \mu\text{m}$  thick. For the future works, the channel geometry to get the appropriate enhancement of CFL for blood plasma separation would be varied as well as an improvement of surface roughness of the constriction channel.

#### REFERENCES

- [1] H. Sharma, D. Nguyen, A. Chen, V. Lew, and M. Khine, "Unconventional Low-Cost Fabrication and Patterning Techniques for Point of Care Diagnostics," *Ann. Biomed. Eng.*, vol. 39, no. 4, pp. 1313–1327, Dec. 2010.
- [2] D. A. Bartholomeusz, R. W. Boutte, and J. D. Andrade, "Xurography: rapid prototyping of microstructures using a cutting plotter," *J. Microelectromechanical Syst.*, vol. 14, no. 6, pp. 1364–1374, Dec. 2005.
- [3] J. Do, J. Y. Zhang, and C. M. Klapperich, "Maskless writing of microfluidics: Rapid prototyping of 3D microfluidics using scratch on a polymer substrate," *Robot. Comput.-Integr. Manuf.*, vol. 27, no. 2, pp. 245–248, Apr. 2011.
- [4] A. C. Glavan, R. V. Martinez, E. J. Maxwell, A. B. Subramaniam, R. M. D. Nunes, S. Soh, and G. M. Whitesides, "Rapid fabrication of pressure-driven open-channel microfluidic devices in omniphobic RF paper," *Lab. Chip*, vol. 13, no. 15, p. 2922, 2013.
- [5] M. Faivre, M. Abkarian, K. Bickraj, and H. A. Stone, "Geometrical focusing of cells in a microfluidic device: An approach to separate blood plasma," *Biorheology*, vol. 43, no. 2, pp. 147–159, Jan. 2006.
- [6] J. Marchalot, Y. Fouillet, and J.-L. Achard, "Multistep microfluidic system for blood plasma separation: architecture and separation efficiency," *Microfluid. Nanofluidics*, vol. 17, no. 1, pp. 167–180, Jul. 2014.
- [7] E. Sollier, H. Rostaing, P. Pouteau, Y. Fouillet, and J.-L. Achard, "Passive microfluidic devices for plasma extraction from whole human blood," *Sens. Actuators B Chem.*, vol. 141, no. 2, pp. 617–624, Sep. 2009.
- [8] S. Prentner, D. M. Allen, L. Larcombe, S. Marson, K. Jenkins, and M. Saumer, "Effects of channel surface finish on blood flow in microfluidic devices," *Microsyst. Technol.*, vol. 16, no. 7, pp. 1091–1096, Jan. 2010.
- [9] R. Arayanarakool, S. Le Gac, and A. van den Berg, "Low-temperature, simple and fast integration technique of microfluidic chips by using a UVcurable adhesive," *Lab. Chip*, vol. 10, no. 16, pp. 2115–2121, 2010